

RESEARCH ARTICLE OPEN ACCESS

Influence of Soil Grain Roughness and Roughness Type on Flow Resistance in Rectangular Rill Channels

Antonino Lucchese¹  | Alessio Nicosia¹  | Vincenzo Palmeri^{1,2}  | Vincenzo Pampalone¹  | Vito Ferro^{1,2} 

¹Department of Agricultural, Food and Forest Sciences, University of Palermo, Palermo, Italy | ²NBFC, National Biodiversity Future Center, Palermo, Italy

Correspondence: Alessio Nicosia (alessio.nicosia@unipa.it)

Received: 2 April 2025 | **Revised:** 9 July 2025 | **Accepted:** 1 August 2025

Funding: The authors received no specific funding for this work.

Keywords: dimensional analysis | flow resistance | rectangular channels | rill erosion | roughness type | self-similarity | soil grain roughness

ABSTRACT

The knowledge of rill flow resistance is required to improve the modelling of upland erosion processes in different hydraulic conditions. Using controlled laboratory conditions, experimental runs in flumes are useful to investigate a specific effect, such as the boundary roughness, on flow resistance. In this paper, the effects of the soil roughness and roughness types on flow resistance are investigated using laboratory measurements. Flow resistance measurements, which were performed for rectangular fixed-bed flumes with different bed and wall arrangements (smooth, covered by a clay-loam, a sandy-loam, a clay soil), were jointly used with literature measurements obtained for rectangular flumes covered by sand or grass. In agreement with previous studies, the analysis showed that, for open-channel rill flows on a fixed bed, the influence of different soil grain roughness on the Darcy–Weisbach friction factor is restrained ($\approx \pm 1\%$). On the other hand, the results highlighted that the effect of a different roughness type (i.e., sand or grass) on flow resistance is appreciable. Ultimately, laboratory measurements of flow resistance in a rectangular cross-section flume are characterised by limited influence of soil grain roughness, and characteristic values of the roughness parameters in the flow resistance equation can be estimated for a non-specific ‘soil roughness’ condition.

1 | Introduction

According to Borrelli et al. (2017), anthropogenic soil uses and related land use changes can be considered responsible for accelerated soil erosion processes. Therefore, soil conservation and land management strategies require information on the characteristics of erosion processes occurring on natural hillslopes and cultivated landscapes (Bennett et al. 2015).

Natural hillslopes are affected by soil erosion processes that produce narrow channels, named rills (Foster et al. 1984; Di Stefano et al. 2022a, 2022b), whose geometry is controlled by hillslope morphology, soil properties, tillage practices, and soil surface roughness. Rills are small channels whose depth varies from some millimetres to several centimetres, which especially occur in steep slopes, and are characterised by sediment transport due

to both the contribution of the interrill areas and scour phenomena shaping the rill wetted perimeter (Foster et al. 1982; Di Stefano et al. 2013).

The intrinsic mechanisms of rill erosion and rill development are related to some hydraulic variables, such as flow velocity, Reynolds number, Froude number and Darcy–Weisbach friction factor (Shen et al. 2016; Nicosia et al. 2022; Li et al. 2024). The characteristics of the rill channel flow affect the erosion processes occurring along these flow paths (Govers et al. 2007), and the knowledge of the hydraulic variables (water depth, flow velocity, roughness) of rill flows is required to develop accurate models of upland erosion processes (Gilley et al. 1990; Di Stefano et al. 2019). The knowledge of the mean rill flow velocity, V , which is related to the hillslope topography, flow discharge, slope steepness and bed surface conditions (Di Stefano

This is an open access article under the terms of the [Creative Commons Attribution](https://creativecommons.org/licenses/by/4.0/) License, which permits use, distribution and reproduction in any medium, provided the original work is properly cited.

© 2025 The Author(s). *Hydrological Processes* published by John Wiley & Sons Ltd.

et al. 2022a), is required to investigate soil entrainment, detachment and transport processes.

The most widespread approach to estimating V is using flow resistance equations (Di Stefano, Ferro, Palmeri, and Pampalone 2017; Carollo et al. 2021), which include a friction factor, such as Manning's n or Darcy–Weisbach f , which is calculated as follows:

$$f = \frac{8gRs}{V^2} \quad (1)$$

where g is the gravitational acceleration, R is the hydraulic radius, and s is the slope gradient. From 1984, many laboratory studies (Foster et al. 1984; Govers 1992; Takken et al. 1998; Giménez and Govers 2001; Peng et al. 2015; Ban et al. 2020) were carried out to determine equations useful for predicting rill flow velocity (Di Stefano et al. 2022a). The main limit of flume investigations is the oversimplification of the controlled conditions as compared to the natural ones, which, however, is very useful to investigate single effects of the studied process. In order to study the effects of grain resistance and sediment transport on rill flow resistance, previous flume investigations were carried out by straight rills having a fixed or a mobile bed channel and a cross-section shape that is generally rectangular (Zhang et al. 2009; Wu et al. 2016; Jiang et al. 2018; Ban et al. 2020; Huang et al. 2020; Ban 2023).

While flume measurements allow the investigation of the uniform flow motion in a straight rill channel with a mobile or fixed bed, field experiments are characterised by a complex rill geometry, which can be studied by accurate 3D models (DTM) created by automatic 3D-photo reconstruction (3D-PR) techniques (Eltner et al. 2015; Frankl et al. 2015; Di Stefano, Ferro, Palmeri, Pampalone, and Agnello 2017; Yang et al. 2021). Recently, Di Stefano et al. (2024) compared rill flume measurements and data obtained in fixed-bed rill channels incised in plots characterised by the same soil roughness. The analysis was developed for two different soils using a theoretical flow resistance equation deduced by Ferro (2017) applying dimensional analysis and the self-similarity condition. The investigation by Di Stefano et al. (2024) established that the influence of different soil roughness on the Darcy–Weisbach friction factor is limited in comparison with the effects due to rill cross-section shape.

However, the scheme of a rectangular cross-section is used for modelling the different rill erosion variables (detachment capacity, rill erosion rate, sediment transport capacity) estimated for a unit of width (Nearing et al. 1989). These rill erosion variables are often tested by experimental investigations carried out by laboratory flumes, and for this reason, the scheme of rectangular rill deserves scientific interest.

Even if Di Stefano et al. (2024) found a limited influence of different soil roughness on the Darcy–Weisbach friction factor, this result, obtained for only two soils, still needs to be assessed to be generalisable. Moreover, studying the effect of different roughness types on flow resistance law, as already made for overland flows by Nicosia et al. (2024), is an interesting topic to be developed for rills. In other words, the main research gaps to

overcome are to assess if the effect of the soil roughness on rill flow resistance is actually negligible, and to investigate the flow resistance behaviour for different roughness types.

The main aim of this investigation is to check the influence of soil roughness on flow resistance, comparing measurements carried out using a rectangular rill channel and different roughness conditions. The experimental runs were performed using a smooth flume and three other flumes covered by soils with different textures (clay-loam, sandy-loam, and clay) and roughness heights ($k_s = 0.119, 0.135, \text{ and } 1.317 \text{ mm}$) to simulate flows moving in fixed bed rills. The measurements performed by Abrantes et al. (2018) for flumes covered by sand and grass were also used with the aim of understanding the discrepancies in flow resistance determined by different roughness types. Therefore, for controlled laboratory conditions and known channel geometry, this study will allow for stating the influence of the soil roughness and roughness type (i.e., sand or grass) on the Darcy–Weisbach friction factor.

2 | Materials and Methods

2.1 | Experimental Measurements of This Investigation and Di Stefano et al. (2024)

The experimental runs were carried out in a sloping flume, 5 m long, 0.04 m deep and 0.078 m wide. A small pipe supplied the discharge entering the flume, and an inflow device with wire meshes, able to spread the flow in the whole flume width and dissipate flow turbulence, was used. At the end of the flume, the water coming out was collected in a tank (Figure 1a). The experimental runs were carried out using a smooth flume and three flumes having bed and walls characterised by different roughness conditions, which were obtained by fixing, with waterproof vinyl glue, sieved soil to the flume bed and walls (Figure 1b). More details of this experimental setup are reported in the paper by Di Stefano et al. (2021).

In particular, one flume was covered by the 'Orleans' clay-loam soil (36.4% sand, 30.9% silt and 32.7% clay), while the others were covered by the 'Aranceto' sandy-loam soil (55.8% sand, 31.4% silt and 12.8% clay) and the 'Sparacia' clay soil (5% sand, 33% silt and 62% clay). The samples of the used soils, which are typical Sicilian soils, were collected from three experimental areas. The particle size distributions of the investigated soils are plotted in Figure 2, and the main characteristics of the investigated soils are listed in Table 1. For each arrangement, the mean roughness height k_s was calculated as the mean height of the solid obtained by the difference between the water volumetric measurements obtained by completely filling the flume with and without roughness. In particular, for the clay arrangement, the mean roughness height was equal to 1.317 mm, while $k_s = 0.135$ and 0.119 mm for the sandy loam and the clay loam ones, respectively.

Each experimental run was characterised by given values of slope s (varying from 0.1% to 15%), discharge Q , and water depth h . The flow discharge was measured by the volumetric technique (i.e., measuring the filling time of a bucket having known volume), while a point gauge placed in the flume axis, 2 m apart from the inlet, and having an accuracy of ± 0.1 mm, was used to measure h . For each run, the hydraulic cross-section area was

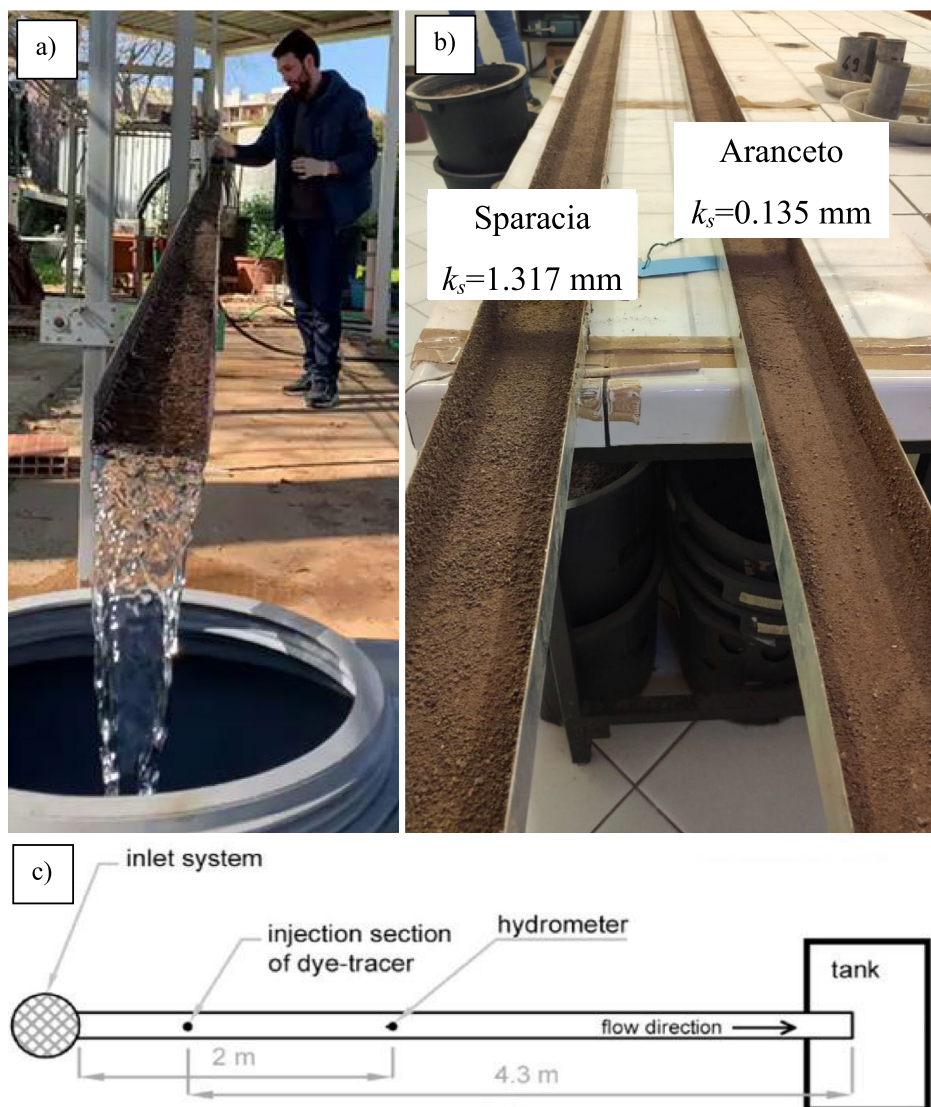


FIGURE 1 | Views of the flume covered by glued sieved soil (a and b) and scheme of the experimental layout (c).

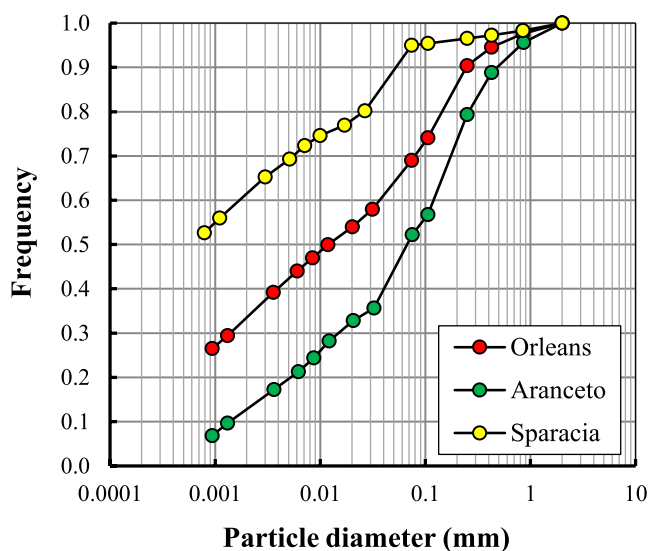


FIGURE 2 | Particle size distribution of the three investigated soils.

calculated by multiplying the measured h and the flow width, and the mean flow velocity V was set equal to the ratio between Q and the cross-section area. The Froude number $F = V/(gh)^{0.5}$, and the Reynolds number $Re = Vh/\nu_k$, in which ν_k is the kinematic viscosity, were also calculated (Table 2).

For the smooth condition, and the ‘Orleans’ and ‘Sparacia’ rough conditions, the flow resistance data are already reported in previous investigations (Di Stefano et al. 2021, 2024; Nicosia, Di Stefano, et al. 2021). In particular, for the smooth configuration, 52 measurements (i.e., 31 data by Di Stefano et al. (2021) and 21 measurements carried out by Di Stefano et al. 2024) were available. For the ‘Orleans’ soil, the total available measurements were 44 (i.e., 24 data by Nicosia, Di Stefano, et al. (2021) and 20 carried out by Di Stefano et al. (2024)), while for the ‘Sparacia’ soil, they were 50 (carried out by Di Stefano et al. (2024)).

The new 50 measurements performed in this investigation were carried out for the ‘Aranceto’ soil using the same 10 slopes (0.1%,

TABLE 1 | Characteristic data of the investigated soils.

Roughness type	Authors	Texture	k_s (mm)	$a, b = 1.1222, c = 0.5927$	$\frac{1.156}{a}$
Smooth	Di Stefano et al. (2024)	—	—	—	—
Orleans	Di Stefano et al. (2024)	Clay loam	0.119	0.3908	2.958
Aranceto	This investigation	Sandy loam	0.135	0.3958	2.920
Sparacia	Di Stefano et al. (2024)	Clay	1.317	0.3971	2.911
Sand	Abrantes et al. (2018)	—	< 1.2	0.3706	—
Synthetic grass	Abrantes et al. (2018)	—	8.5	0.3649	—
Smooth	Abrantes et al. (2018)	—	—	0.3703	—

1.0%, 2.5%, 4.4%, 6.1%, 8.7%, 9.0%, 11.0%, 13.0% and 15.0%) (Table 2) investigated by Di Stefano et al. (2024).

2.2 | Literature Measurements by Abrantes et al. (2018)

Abrantes et al. (2018) performed flow measurements using a sloping hydraulic channel 3 m long and 0.15 m wide equipped with a water recirculation circuit with a 500 L reservoir, a pump, and a flow control valve. The channel bed and walls were made of smooth transparent acrylic sheets, while inflow and outflow were free; consequently, flow velocity and depth were controlled by the flow discharge, bed slope and bed surface roughness. Abrantes et al. (2018) carried out flow velocity measurements for four different bed roughness types (smooth acrylic, sand, stones and synthetic grass). In the present investigation, the data obtained for the smooth, sand, and synthetic grass conditions were used. The smooth acrylic runs were conducted on the smooth acrylic sheet of the channel bed. The sand runs were performed by placing an acrylic board with homogeneously glued sieved sand particles (diameter < 1.2 mm). The synthetic grass runs were carried out after fixing a synthetic grass carpet (8.5 mm height) to the channel bed. For each roughness type, three bed slopes (0.8%, 4.4% and 13.2%) were tested. Abrantes et al. (2018) measured flow velocity in triplicate using the triple tracer and flow depth by a precision limnimeter. The flow discharge (in the range 0.032–1.813 L s⁻¹) was controlled manually by the flow control valve and measured at the channel outlet by the volumetric method.

2.3 | Theoretical Flow Resistance Equation

Physically-based or process-oriented models for estimating soil loss use classical hydraulic equations, such as Manning, Darcy–Weisbach, and Chezy's equations (Nouwakpo et al. 2016; Nicosia and Ferro 2023), even if they were established and calibrated for stream/river conditions. According to Ferro (2017), the flow-resistance law can be obtained by integrating the flow-velocity distribution, whose power shape is obtained by applying the dimensional analysis and the self-similarity condition in the cross-section. The vertical velocity distribution of a uniform turbulent

open-channel flow (Ferro and Porto 2018) can be represented by the following (Barenblatt 1979, 1987; Carollo et al. 2021):

$$\frac{v}{u_*} = \Gamma \left(\frac{u_* y}{\nu_k} \right)^\delta \quad (2)$$

where v is the local velocity, y is the distance from the bottom, $u_* = \sqrt{g R s}$ is the shear velocity, Γ is a function estimated by velocity measurements, and δ is an exponent calculated by the following equation (Castaing et al. 1990):

$$\delta = \frac{1.5}{\ln Re} \quad (3)$$

Integrating Equation (2), the following expression of the Darcy–Weisbach friction factor f is obtained (Ferro and Porto 2018):

$$f = 8 \left[\frac{(\delta + 1)(\delta + 2)}{2^{1-\delta} \Gamma Re^\delta} \right]^{2/(1+\delta)} \quad (4)$$

If the distance from the bottom in which the local velocity v is equal to V is set $y = \alpha h$, the following equation is obtained by Equation (2) (Ferro 2017):

$$\Gamma_v = \frac{V}{u_* \left(\frac{u_* \alpha h}{\nu_k} \right)^\delta} \quad (5)$$

where Γ_v is the Γ value calculated by the measurements of V , R , h and s ; $\alpha < 1$ is a coefficient, dependent on δ , considering that V is located below the water surface and only one velocity profile is used to represent the velocity distribution for the whole cross-section (Ferro 2017).

The coefficient α is calculated by the following theoretical relationship (Ferro 2017):

$$\alpha = \left[\frac{2^{1-\delta}}{(\delta + 1)(\delta + 2)} \right]^{1/\delta} \quad (6)$$

As Γ theoretically depends only on the channel slope, Reynolds number and Froude number, Γ_v can be estimated by the following equation (Ferro 2018):

TABLE 2 | Characteristic data (discharge Q , slope s , water depth h , Reynolds number Re and Froude number F) of the experimental runs carried out for the 'Aranceto' configuration and a slope range 0.1%–15%.

Q (Ls^{-1})	s (%)	h (m)	Re	F
0.26	0.1	0.014	3001	0.62
0.39	0.1	0.019	4501	0.63
0.50	0.1	0.022	5771	0.63
0.60	0.1	0.023	6925	0.72
0.80	0.1	0.029	9233	0.65
0.24	1	0.012	2770	0.72
0.37	1	0.015	4270	0.82
0.58	1	0.020	6694	0.87
0.68	1	0.021	7848	0.90
0.78	1	0.023	9003	0.90
0.21	2.5	0.009	2366	1.02
0.39	2.5	0.012	4501	1.17
0.55	2.5	0.014	6348	1.42
0.70	2.5	0.017	8056	1.34
0.85	2.5	0.021	9811	1.18
0.22	4.4	0.009	2539	1.13
0.38	4.4	0.011	4386	1.41
0.61	4.4	0.014	7041	1.49
0.71	4.4	0.015	8195	1.52
0.82	4.4	0.017	9464	1.53
0.22	6.1	0.009	2493	1.07
0.36	6.1	0.011	4155	1.31
0.50	6.1	0.013	5771	1.41
0.76	6.1	0.015	8772	1.76
0.84	6.1	0.016	9695	1.75
0.32	8.7	0.009	3647	1.54
0.45	8.7	0.010	5194	1.90
0.64	8.7	0.011	7387	2.33
0.74	8.7	0.013	8541	2.00
0.85	8.7	0.014	9811	2.15
0.36	9	0.010	4155	1.54
0.47	9	0.011	5425	1.79
0.58	9	0.012	6694	1.81
0.63	9	0.013	7271	1.70
0.86	9	0.016	9926	1.82
0.29	11	0.008	3347	1.83

(Continues)

TABLE 2 | (Continued)

Q (Ls^{-1})	s (%)	h (m)	Re	F
0.46	11	0.010	5309	1.91
0.57	11	0.011	6579	2.00
0.70	11	0.014	8079	1.81
0.82	11	0.015	9464	1.88
0.29	13	0.007	3347	1.98
0.44	13	0.010	5021	1.92
0.55	13	0.010	6394	2.17
0.63	13	0.011	7271	2.30
0.80	13	0.012	9222	2.49
0.37	15	0.009	4270	1.66
0.45	15	0.010	5194	1.90
0.59	15	0.011	6810	2.07
0.74	15	0.013	8541	2.09
0.87	15	0.014	10041	2.10

$$\Gamma_v = a \frac{F^b}{s^c} \quad (7)$$

in which a , b and c are coefficients estimated by the available measurements.

3 | Results

For the smooth flume, as reported by Di Stefano et al. (2024), the measurements of Reynolds (from 3018 to 8751) and Froude (from 1.44 to 7.67) numbers always correspond to turbulent flow regimes and supercritical flows. For the investigated rough rill channels, the measurements of Reynolds and Froude numbers correspond to transitional and turbulent flow regimes ($1911 \leq Re \leq 10247$) and subcritical and supercritical flows ($0.46 < F \leq 2.88$) (Figure 3).

Firstly, the measurements carried out for the three different soils (Orleans, Aranceto and Sparacia) were represented by the $f-\Gamma_v$ plot (Figure 4), in which Γ_v are the measured values obtained by Equation (5). The plotted pairs demonstrate that a strong relationship exists between the measured values of the Darcy–Weisbach friction factor and the Γ_v function, which for a given soil roughness depends on the measured values of s , V and h . For the investigated soil roughnesses, Figure 4 highlights that negligible differences in the measured Darcy–Weisbach friction factors occur for the three investigated soils.

At first, Equation (7) was calibrated using the measurement of the smooth arrangement, and the coefficients a (0.3745), b (1.1222) and c (0.5927) were obtained (Table 1). Figure 5 shows, for the smooth arrangement, the good agreement

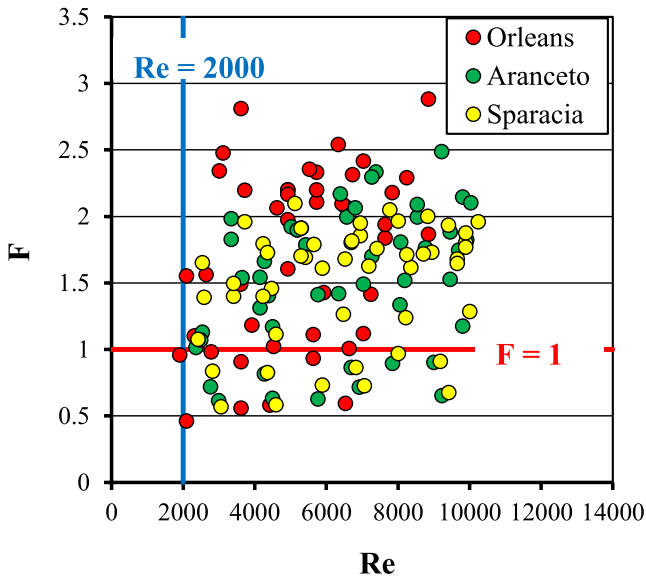


FIGURE 3 | Relationship between the Froude and Reynolds numbers for the three investigated soils.

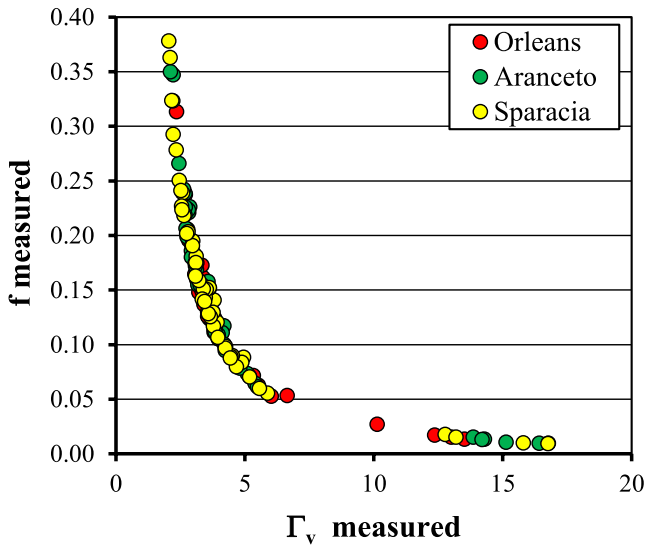


FIGURE 4 | Relationship between the measured f values and Γ_v (Equation 5) for the three investigated soils.

between the measured f values and those calculated by introducing Equation (7) with $a = 0.3745$, $b = 1.1222$ and $c = 0.5927$ into Equation (4).

Considering that the Froude number and slope are variables representative of the rill flow, the use of a constant value of the exponents b and c of Equation (7) (Nicosia, Bischetti, et al. 2021; Nicosia et al. 2023), equal to the values obtained for the smooth arrangement (Table 1), allows for using the single coefficient a to express the effect of soil roughness according to the following relationship:

$$\Gamma_v = a \frac{F^{1.1222}}{s^{0.5927}} = a X \quad (8)$$

Successively, the behaviour of the pairs $(\Gamma_v, X = F^{1.1222} s^{-0.5927})$ (Figure 6) was investigated and, for each soil, the a coefficient, equal to the slope coefficient of the best-fit straight line passing through the origin of the axes, was determined (Table 1).

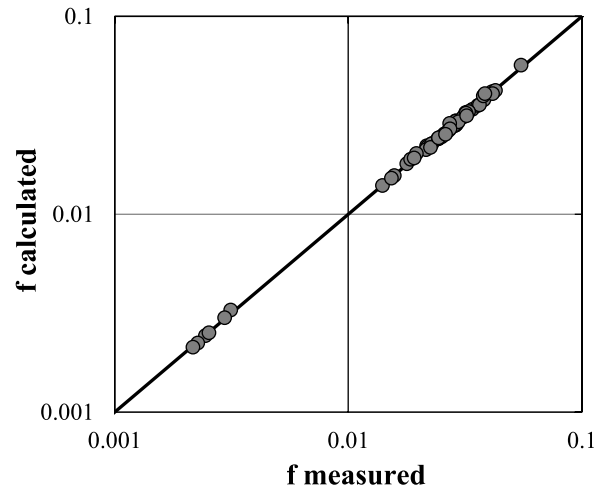


FIGURE 5 | Comparison between the measured f values and those calculated introducing Equation (7) with $a = 0.3745$, $b = 1.1222$ and $c = 0.5927$ into Equation (4).

The comparison between the measured Γ_v values, obtained by Equation (5), and those calculated by Equation (8) is plotted in Figure 7a. Figure 7b shows the comparison between the measured f values and those calculated by Equation (4) coupled with Equation (8).

By coupling Equation (4) with Equation (8), the following flow resistance equation is obtained:

$$f = 8 \left[\frac{(\delta + 1)(\delta + 2)}{2^{1-\delta} 4.4817} \right]^{\frac{2}{1+\delta}} \left[\frac{s^{0.5927}}{a F^{1.1222}} \right]^{\frac{2}{1+\delta}} \quad (9)$$

Considering that δ varies within a narrow range (0.162–0.198), its mean value (0.174) can be introduced into Equation (9); and the following equation is deduced:

$$f = \left(\frac{1.156}{a} \right) \frac{s^{1.0097}}{F^{1.9117}} \quad (10)$$

in which the coefficient $1.156/a$ ranges from 2.911 (Sparacia, clay soil) to 2.957 (Orleans, clay-loam soil (Table 1)). For given morphological (slope, rectangular cross-section, fixed bed) and hydraulic conditions (Froude number), the use of the mean value of $1.156/a$, equal to 2.929, independent of soil texture, determines a friction factor overestimation of 0.96% for the Orleans soil and an underestimation of -0.32% and -0.64% for the Sparacia and Aranceto soils, respectively. In other words, for given morphological and hydraulic conditions and using the mean value of $1.156/a$, equal to 2.929, the effect of a different soil is always less than $\pm 1\%$.

For the rough rectangular channels (Orleans, Aranceto and Sparacia soils), the errors E in the f estimate (Equation 9 with the a coefficients listed in Table 1) (Figure 8) are less than or equal to $\pm 7\%$ for 62.5% of the cases and are less than or equal to $\pm 9\%$ for 98.6% of the cases.

Figure 9, which compares the behaviour of the pairs $(\Gamma_v, X = F^{1.1222} s^{-0.5927})$ for the smooth arrangement investigated by Abrantes et al. (2018) with that of the measurements on a smooth bed by Di Stefano et al. (2024) (used to determine b and

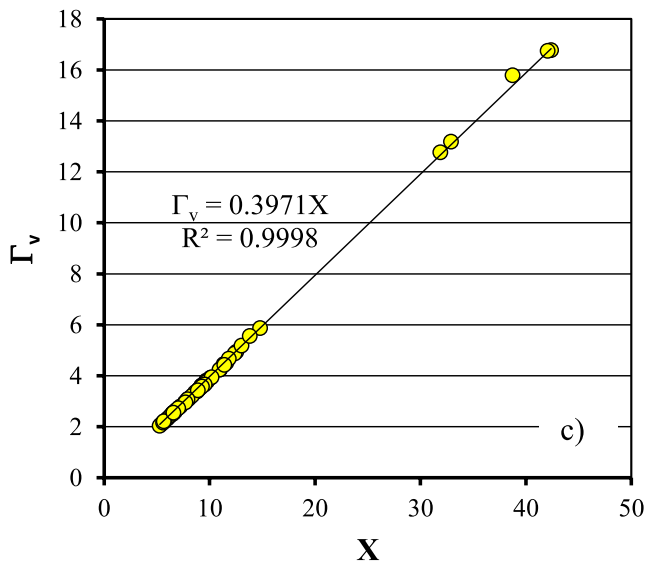
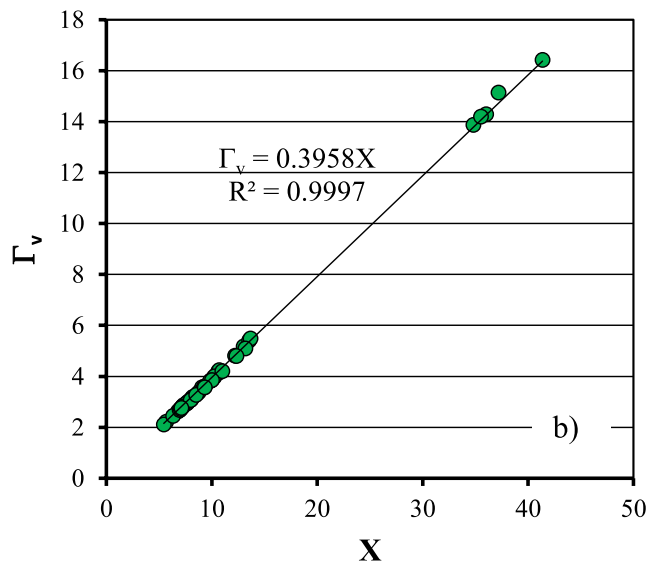
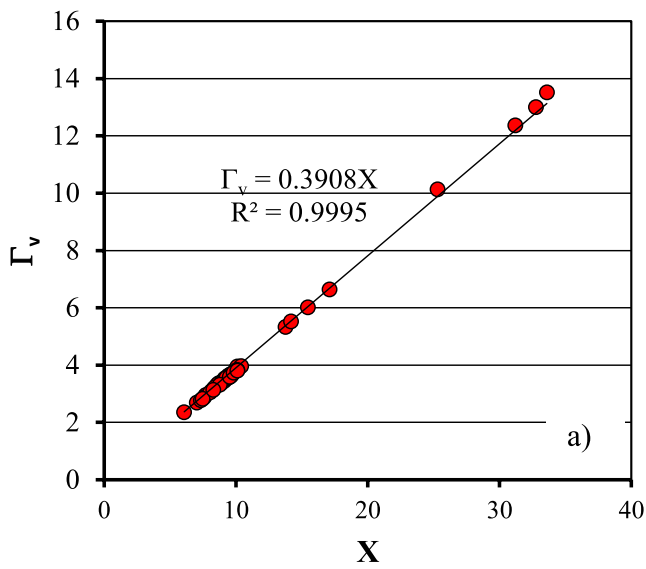


FIGURE 6 | Pairs (X, Γ_v) for the three investigated soils (a) Orleans, (b) Aranceto and (c) Sparacia.

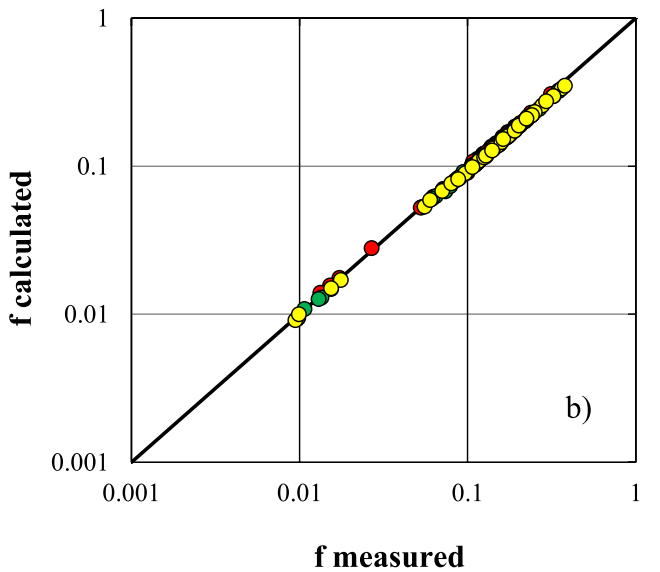
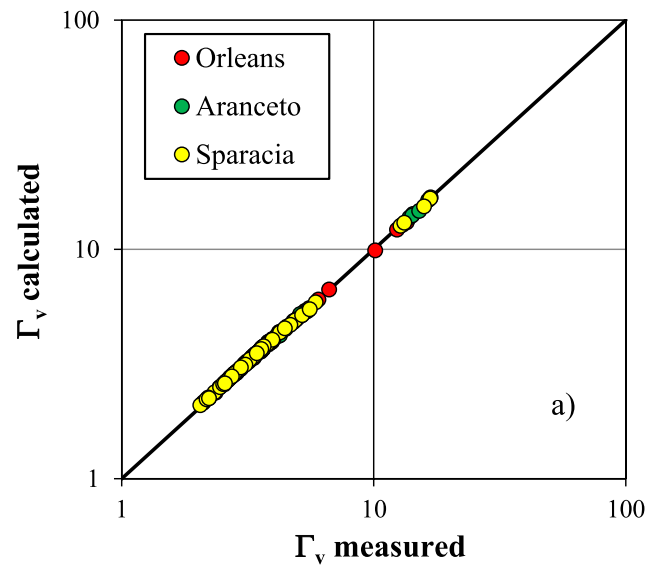


FIGURE 7 | Comparison between the measured Γ_v values, obtained by Equation (5), and those calculated by Equation (8) (a) and between the measured f values and those calculated by Equation (4) and Equation (8) (b).

c coefficients of Equation (8)), demonstrates that the data by Abrantes et al. (2018) behave in the same way as those used in this investigation; thus, they can be used in order to assess the influence of the roughness type on flow resistance.

Figure 10 shows the behaviour of the pairs $(\Gamma_v, X = F^{1.1222} s^{-0.5927})$ for the sand (Figure 10a) and synthetic grass (Figure 10b) arrangements investigated by Abrantes et al. (2018), from which the a coefficients, equal to the slope coefficient of the best-fit straight line passing through the origin of the axes, were determined (Table 1). Considering the mean a value characterising the three soil arrangements (0.3945), the a coefficients obtained for the sand (0.3706) and the synthetic grass (0.3649) arrangements represent 93.93% and 92.48%, respectively. In other words, the different roughness types determine a more

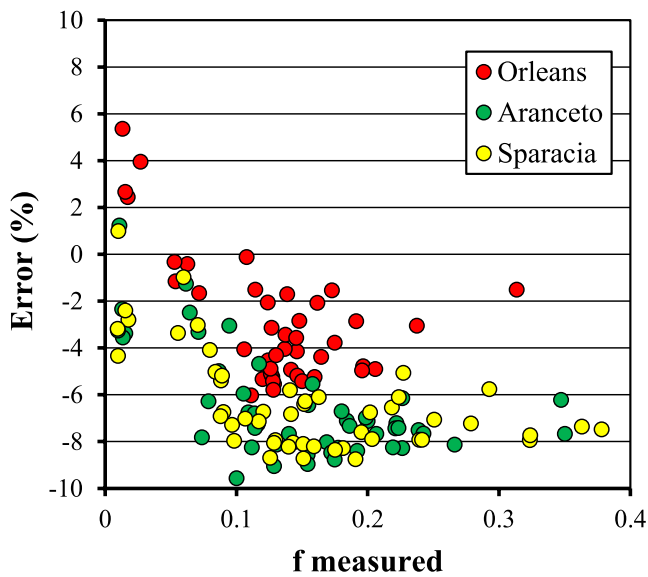


FIGURE 8 | Estimate errors of the Darcy–Weisbach friction factor, in the range of the measured f values, for the three investigated soils.

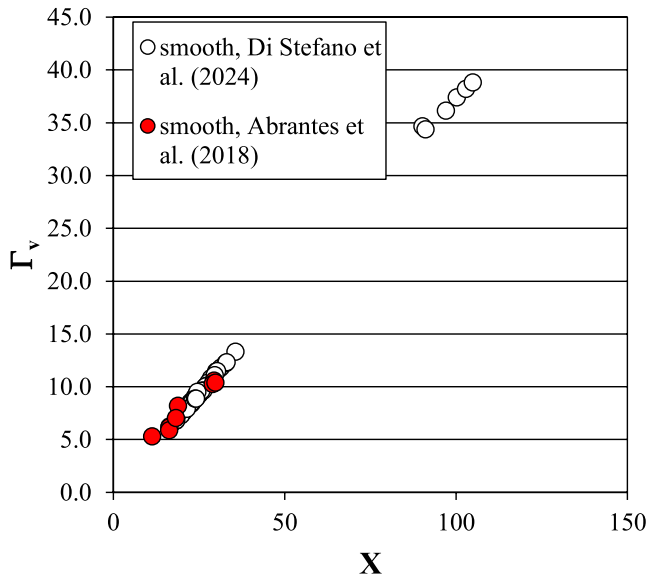


FIGURE 9 | Pairs $(\Gamma_v, X = F^{1.1222} s^{-0.5927})$ for the smooth arrangement investigated by Di Stefano et al. (2024) and Abrantes et al. (2018).

significant (-6.07% and -7.52%) variation of Γ_v as compared to the investigated soils.

4 | Discussion

The result shown in Figure 5 demonstrates that the flow resistance law (Equation 7 with $a = 0.3745$, $b = 1.1222$ and $c = 0.5927$ into Equation 4) gives an accurate estimate of the Darcy–Weisbach friction factor values for the smooth arrangement. Even using fixed b and c values obtained for the smooth arrangement and attributing the effect of soil roughness only to the a coefficient (Equation 8 with a coefficient listed in Table 1) for the rough bed data, the flow resistance equation (Equation 4) is characterised by good performance (Figure 7b). Figure 8 demonstrates that using exponents $b = 1.1222$ and $c = 0.5927$

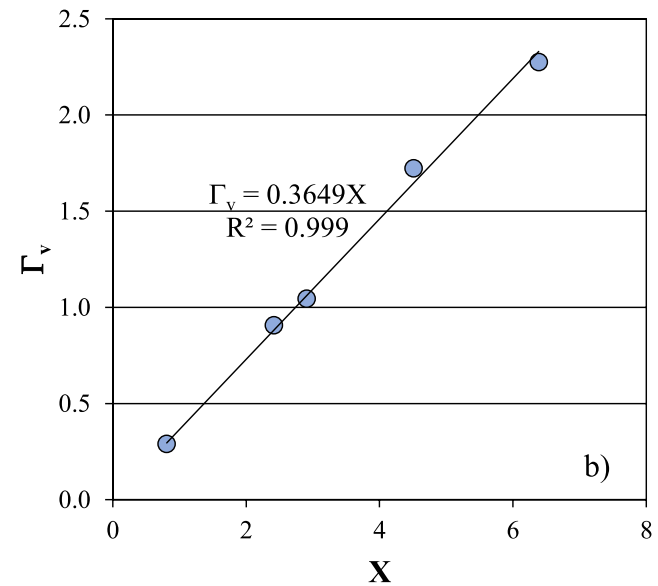
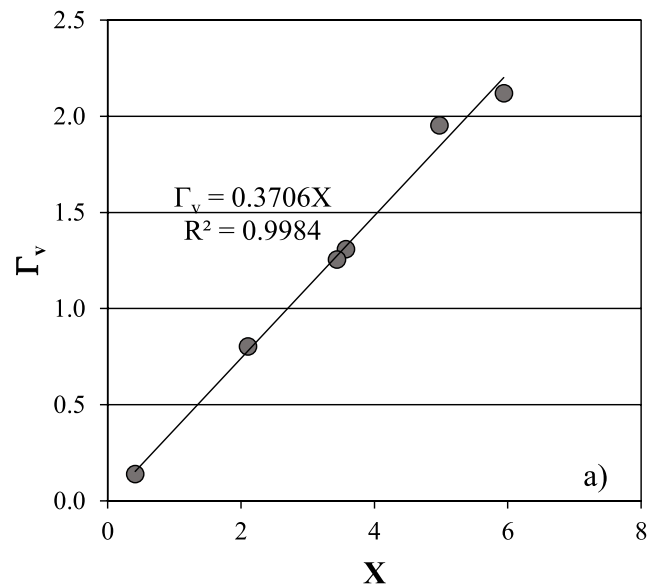


FIGURE 10 | Pairs $(\Gamma_v, X = F^{1.1222} s^{-0.5927})$ for the sand (a) and synthetic grass (b) arrangements investigated by Abrantes et al. (2018).

determines low errors, which, however, pointed out a systematic underestimation of the friction factors for the highest f values. This result could be dependent on a low residual effect of soil roughness on the b and c exponents.

It is worth noting that the obtained a values of Equation (8) (Table 1) for the three investigated soils are very similar. Moreover, the analysis performed by Equation (10) underlined that, for given morphological and hydraulic conditions, the use of the mean value of $1.156/a$ (2.929) determines a negligible effect (always less than $\pm 1\%$) on the friction factor estimation performance. These results point out that the actual influence of soil roughness is negligible, in agreement with the findings by Di Stefano et al. (2024), who found that ‘..... for a fixed-bed channel, the effect of the cross-section shape on the Darcy–Weisbach friction factor is much greater than that due to the soil grain size roughness’. Therefore, the application of Equation (10) can be performed using an a value simply representing the category

'soil', regardless of the soil texture. In other words, the change due to the roughness height of different soils does not appreciably affect the estimate of the a coefficient.

Instead, the results obtained for the sand and synthetic grass data (Table 1) by Abrantes et al. (2018) highlight that a different a value accounting for the roughness type determines more relevant differences in Γ_v , and thus in the Darcy–Weisbach friction factor. These results imply that, while a different soil grain roughness does not produce a substantial effect on flow resistance, a different roughness type affects more appreciably flow resistance.

The main implication of this work is that the flow resistance results deduced by laboratory measurements with regular cross-sections, thus neglecting a complex geometry, limit the effects of the soil roughness. In other words, even if laboratory measurements are useful to investigate the effect of a single variable as soil roughness, these measurements are also affected by the oversimplifications of the controlled conditions and imply the risk of representing conditions that are far from the natural field ones.

On the other hand, the findings of this investigation testify that the influence of the roughness type (soil, sand, grass) on flow resistance is appreciable. In conclusion, this work demonstrates that laboratory experiments using a rectangular cross-section allow for appreciating the differences between different roughness types, but not those ascribable to soil grain roughness.

This work has the limit of testing a single value of the flume width for the runs performed with the soil arrangements. Therefore, a future research challenge should be to carry out other experimental runs using soil roughened flumes characterised by different widths, representative of the rill width variability.

5 | Conclusions

The cross-sectional shape is useful information for calculating rill volume and estimating the main hydraulic variables. In the past, flume investigations were widely used to investigate schematized conditions useful to study the effect of a single rill variable.

In this investigation, flow resistance measurements carried out for a smooth flume and the other three covered by a clay-loam, a sandy-loam, and a clay soil were compared. Literature measurements obtained for a rectangular flume covered by sand and another one by grass were also used. The analysis showed that the effect of different soil grain roughness on the Darcy–Weisbach friction factor is low (lower than $\pm 1\%$ for a rectangular channel), confirming the previous results by Di Stefano et al. (2024). Instead, the results highlighted that the influence of the roughness type on flow resistance is appreciable. Therefore, for an open-channel flow on a fixed bed having a rectangular cross-section, the effect of the soil grain size roughness on the friction factor is limited, while the effect ascribable to a different roughness type is appreciable.

Acknowledgements

All authors contributed to outline the investigation, analyse the data, discuss the results, and write the manuscript. This research did not receive any specific grant from funding agencies in the public, commercial, or not-for-profit sectors. Open access publishing facilitated by Università degli Studi di Palermo, as part of the Wiley - CRUI-CARE agreement.

Conflicts of Interest

The authors declare no conflicts of interest.

Data Availability Statement

The data that support the findings of this study are openly available in Mendeley at <https://data.mendeley.com/datasets/v47nn9xbkr/1>.

References

- Abrantes, J. R., R. B. Moruzzi, A. Silveira, and J. L. de Lima. 2018. "Comparison of Thermal, Salt and Dye Tracing to Estimate Shallow Flow Velocities: Novel Triple-Tracer Approach." *Journal of Hydrology* 557: 362–377.
- Ban, Y. 2023. "Measurements and Estimation of Flow Velocity in Mobile Bed Rills." *International Journal of Sediment Research* 38, no. 1: 97–104.
- Ban, Y. Y., W. Wang, and T. W. Lei. 2020. "Measurement of Rill and Ephemeral Gully Flow Velocities and Their Model Expression Affected by Flow Rate and Slope Gradient." *Journal of Hydrology* 589: 125172.
- Barenblatt, G. I. 1979. *Similarity, Self-Similarity, and Intermediate Asymptotics*, 218. Consultants Bureau Plenum Press.
- Barenblatt, G. I. 1987. *Dimensional Analysis*. Gordon & Breach, Science Publishers Inc.
- Bennett, S. J., L. M. Gordon, V. Neroni, and R. R. Wells. 2015. "Emergence, Persistence, and Organization of Rill Networks on a Soil-Mantled Experimental Landscape." *Natural Hazards* 79: 7–24. <https://doi.org/10.1007/s11069-015-1599-8>.
- Borrelli, P., D. A. Robinson, L. R. Fleischer, et al. 2017. "An Assessment of the Global Impact of 21st Century Land Use Change on Soil Erosion." *Nature Communications* 8: 2013. <https://doi.org/10.1038/s41467-017-02142-7>.
- Carollo, F. G., C. Di Stefano, A. Nicosia, V. Palmeri, V. Pampalone, and V. Ferro. 2021. "Flow Resistance in Mobile Bed Rills Shaped in Soils With Different Texture." *European Journal of Soil Science* 72: 2062–2075.
- Castaing, B., Y. Gagne, and E. J. Hopfinger. 1990. "Velocity Probability Density Functions of High Reynolds Number Turbulence." *Physica D: Nonlinear Phenomena* 46: 177–200.
- Di Stefano, C., V. Ferro, V. Palmeri, and V. Pampalone. 2017. "Flow Resistance Equation for Rills." *Hydrological Processes* 31: 2793–2801. <https://doi.org/10.1002/hyp.11221>.
- Di Stefano, C., V. Ferro, V. Palmeri, V. Pampalone, and F. Agnello. 2017. "Testing the Use of an Image-Based Technique to Measure Gully Erosion at Sparacia Experimental Area." *Hydrological Processes* 31: 573–585.
- Di Stefano, C., V. Ferro, V. Pampalone, and F. Sanzone. 2013. "Field Investigation of Rill and Ephemeral Gully Erosion in the Sparacia Experimental Area, South Italy." *Catena* 101: 226–234.
- Di Stefano, C., A. Nicosia, V. Palmeri, V. Pampalone, and V. Ferro. 2021. "Flume Experiments for Assessing the Dye-Tracing Technique in Rill Flows." *Flow Measurement and Instrumentation* 77, no. 2: 101870.

- Di Stefano, C., A. Nicosia, V. Palmeri, V. Pampalone, and V. Ferro. 2022a. "Rill Flow Velocity and Resistance Law: A Review." *Earth-Science Reviews* 231: 104092.
- Di Stefano, C., A. Nicosia, V. Palmeri, V. Pampalone, and V. Ferro. 2022b. "Rill Flow Resistance Law Under Sediment Transport." *Journal of Soils and Sediments* 22: 334–347. <https://doi.org/10.1007/s11368-021-03083-x>.
- Di Stefano, C., A. Nicosia, V. Pampalone, V. Palmeri, and V. Ferro. 2019. "New Technique for Measuring Water Depth in Rill Channels." *Catena* 181: 104090.
- Di Stefano, C., A. Nicosia, V. Pampalone, V. Palmeri, and V. Ferro. 2024. "Evaluating the Effects of Soil Grain Roughness and Rill Cross-Section Shape on Flow Resistance." *Hydrological Processes* 38, no. 4: e15119.
- Eltner, A., P. Baumgart, H. G. Maas, and D. Faust. 2015. "Multi-Temporal UAV Data for Automatic Measurement of Rill and Interrill Erosion on Loess Soil." *Earth Surface Processes and Landforms* 40, no. 6: 741–755. <https://doi.org/10.1002/esp.3673>.
- Ferro, V. 2017. "New Flow Resistance Law for Steep Mountain Streams Based on Velocity Profile." *Journal of Irrigation and Drainage Engineering* 143, no. 8: 1–6.
- Ferro, V. 2018. "Flow Resistance Law Under Equilibrium Bed-Load Transport Conditions." *Flow Measurement and Instrumentation* 64: 1–8. <https://doi.org/10.1016/j.flowmeasinst.2018.10.008>.
- Ferro, V., and P. Porto. 2018. "Applying Hypothesis of Self-Similarity for Flow Resistance Law in Calabrian Gravel Bed Rivers (Fiumare)." *Journal of Hydraulic Engineering* 144: 1–11.
- Foster, G. R., L. F. Huggins, and L. D. Meyer. 1984. "A Laboratory Study of Rill Hydraulics: I. Velocity Relationships." *Transactions of ASAE* 27: 790–796.
- Foster, G. R., F. Lombardi, and W. C. Moldenhauer. 1982. "Evaluation of Rainfall-Runoff Erosivity Factors for Individual Storms." *Transactions of ASAE* 25, no. 1: 124–129. <https://doi.org/10.13031/2013.33490>.
- Frankl, A., C. Stal, A. Abraha, et al. 2015. "Detailed Recording of Gully Morphology in 3D Through Image-Based Modelling." *Catena* 127: 92–101.
- Gilley, J. E., E. R. Kottwitz, and J. R. Simanton. 1990. "Hydraulics Characteristics of Rills." *Transactions of ASAE* 27: 797–804.
- Giménez, R., and G. Govers. 2001. "Interaction Between Bed Roughness and Flow Hydraulics in Eroding Rills." *Water Resources Research* 37: 791–799.
- Govers, G. 1992. "Relationship Between Discharge, Velocity and Flow Area for Rills Eroding Loose, Non-Layered Materials." *Earth Surface Processes and Landforms* 17: 515–528.
- Govers, G., R. Giménez, and K. Van Oost. 2007. "Rill Erosion: Exploring the Relationship Between Experiments, Modeling and Field Observations." *Earth-Science Reviews* 83: 87–102.
- Huang, Y., F. Li, Z. Liu, J. Li, and X. Gao. 2020. "Experimental Determination of Sediment Transport Capacity of Concentrated Water Flow Over Saturated Soil Slope." *European Journal of Soil Science* 72, no. 2: 756–768.
- Jiang, F., P. Gao, X. Si, et al. 2018. "Modelling the Sediment Transport Capacity of Flows in Non-Erodible Rills." *Hydrometallurgy Process* 32, no. 26: 3852–3865. <https://doi.org/10.1002/hyp.13294>.
- Li, D., X. Chen, W. Tan, et al. 2024. "Response of Erosion Rate to Hydrodynamic Parameters in Sheet and Rill Erosion Process on Saturated Soil Slopes." *Soil & Tillage Research* 237: 105996.
- Nearing, M. A., G. R. Foster, L. J. Lane, and S. C. Finkner. 1989. "A Process-Based Soil Erosion Model for USDA-Water Erosion Prediction Project." *Transactions of ASAE* 32, no. 5: 1587–1593.
- Nicosia, A., G. B. Bischetti, E. Chiaradia, C. Gandolfi, and V. Ferro. 2021. "A Full-Scale Study of Darcy-Weisbach Friction Factor for Channels Vegetated by Riparian Species." *Hydrological Processes* 35: e14009. <https://doi.org/10.1002/hyp.14009>.
- Nicosia, A., C. Di Stefano, V. Palmeri, V. Pampalone, and V. Ferro. 2021. "Roughness Effect on the Correction Factor of Surface Velocity for Rill Flows." *Hydrological Processes* 35: e14407. <https://doi.org/10.1002/hyp.14407>.
- Nicosia, A., C. Di Stefano, V. Palmeri, M. A. Serio, and V. Ferro. 2024. "Assessing a Transitional and Turbulent Overland Flow Resistance Law for Surfaces With Different Roughness." *Journal of Hydrology* 641: 131858.
- Nicosia, A., and V. Ferro. 2023. "Flow Resistance due to Shrubs and Woody Vegetation." *Flow Measurement and Instrumentation* 89: 102308. <https://doi.org/10.1016/j.flowmeasinst.2023.102308>.
- Nicosia, A., V. Palmeri, and V. Ferro. 2023. "Flow Resistance Law in Channels With Emergent Rigid Vegetation." *Ecohydrology* 17, no. 5: e2646. <https://doi.org/10.1002/eco.2646>.
- Nicosia, A., V. Palmeri, V. Pampalone, C. Di Stefano, and V. Ferro. 2022. "Slope Threshold in Rill Flow Resistance." *Catena* 208: 105789.
- Nouwakpo, S. K., C. J. Williams, O. Z. Al-Hamdani, M. A. Weltz, F. Pierson, and M. A. Nearing. 2016. "A Review of Concentrated Flow Erosion Processes on Rangelands: Fundamental Understanding and Knowledge Gaps." *International Soil and Water Conservation Research* 4: 75–86.
- Peng, W., Z. Zhang, and K. Zhang. 2015. "Hydrodynamic Characteristics of Rill Flow on Steep Slopes." *Hydrological Processes* 29: 3677–3686.
- Shen, H., F. Zheng, L. Wen, Y. Han, and W. Hu. 2016. "Impact of Rainfall Intensity and Slope Gradient on Rill Erosion Processes at Loessial Hillslope." *Soil & Tillage Research* 155: 429–436.
- Takken, I., G. Govers, C. A. A. Ciesiolka, D. M. Silburn, and R. J. Loch. 1998. "Factors Influencing the Velocity-Discharge Relationship in Rills." *Modeling Soil Erosion, Sediment Transport and Closely Related Hydrology Process* 249: 63–69.
- Wu, B., Z. Wang, N. Shen, and S. Wang. 2016. "Modelling Sediment Transport Capacity of Rill Flow for Loess Sediments on Steep Slopes." *Catena* 147: 453–462.
- Yang, Y., Y. Shi, X. Liang, T. Huang, S. Fu, and B. Liu. 2021. "Evaluation of Structure From Motion (SfM) Photogrammetry on the Measurement of Rill and Interrill Erosion in a Typical Loess." *Geomorphology* 385: 107734. <https://doi.org/10.1016/j.geomorph.2021.107734>.
- Zhang, G. H., Y. M. Liu, Y. F. Han, and X. H. Zhang. 2009. "Sediment Transport and Soil Detachment on Steep Slopes: I. Transport Capacity Estimation." *Soil Science Society of America Journal* 73, no. 4: 1291–1297.